

## Supplementary Information

# Controlling the stereospecific bonding motif of Au-thiolate links

*Luciano Colazzo,<sup>\*,1,2,†</sup> Mohammed S. G. Mohammed,<sup>1,2</sup> Aurelio Gallardo,<sup>3</sup> Zakaria M. Abd El-Fattah,<sup>4</sup> José A. Pomposo,<sup>2,5,6</sup> Pavel Jelinek,<sup>3</sup> Dimas G. de Oteyza<sup>\*,1,2,5</sup>*

<sup>1</sup>Donostia International Physics Center, 20018 San Sebastián, Spain.

<sup>2</sup>Centro de Física de Materiales (CFM-MPC), CSIC-UPV/EHU, 20018 San Sebastián, Spain.

<sup>3</sup>Institute of Physics, The Czech Academy of Sciences, 162 00 Prague, Czech Republic.

<sup>4</sup>Physics Department, Faculty of Science, al-Azhar University, Nasr City E-11884 Cairo, Egypt

<sup>5</sup>Ikerbasque, Basque Foundation for Science, Bilbao, Spain.

<sup>6</sup>Departamento de Física de Materiales, Universidad del País Vasco (UPV/EHU), Apartado 1072, E-20800 San Sebastián, Spain.

### Calculations of different BMB trimer structures

The bonding between the BMB molecules has been studied theoretically by means of DFT calculations. Two structures, with the molecules connected through thiolate-Au and disulfide bonds, were considered. The relaxed structures are shown in figure S1. The formation of the structures connected by S-Au-S is found to be around 5 eV more favorable than the S-S linked one. The interaction between molecules in absence of adatoms is hard to attain, since the molecules tend to stay linked mainly with the substrate. This is reflected in the relaxed structure of three BMB molecules put close each other trying to form a BMB<sub>3</sub> compound by S-S linkers (Figure S1b). In this scenario the molecules repels each other and links the S atoms to the substrate, with a S-S distance of 4.77 Å in average, while the distance between the sulfur and substrate atoms is 2.58 Å in average. In addition, as readily commented in the main text, the structure with S-Au-S links agrees much better with the structure observed experimentally.

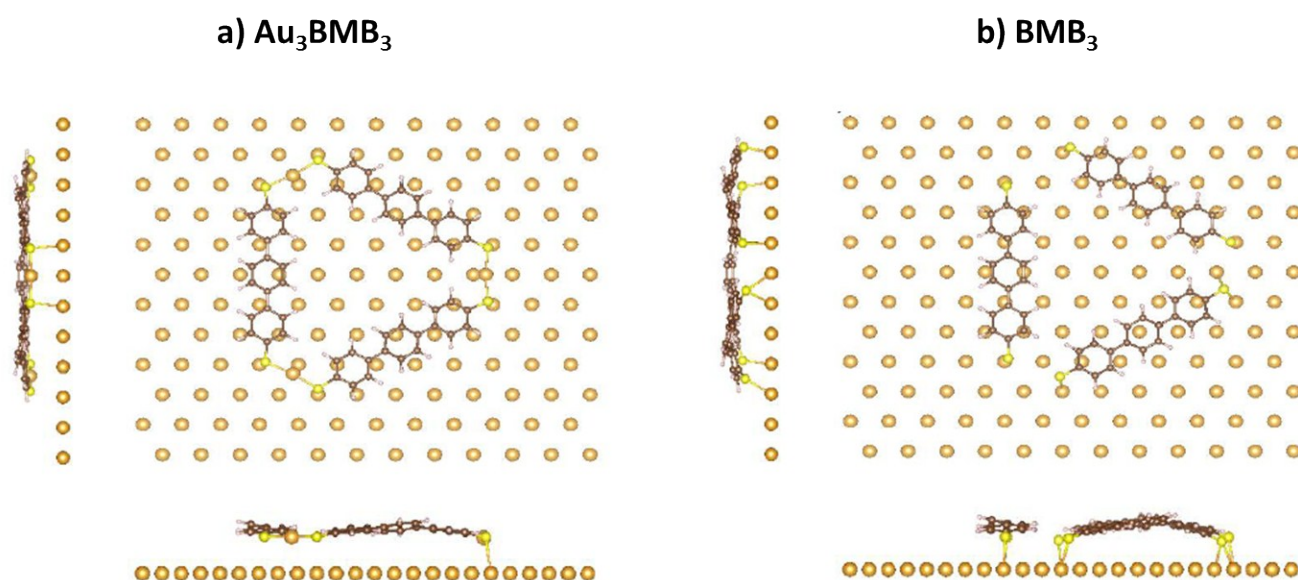
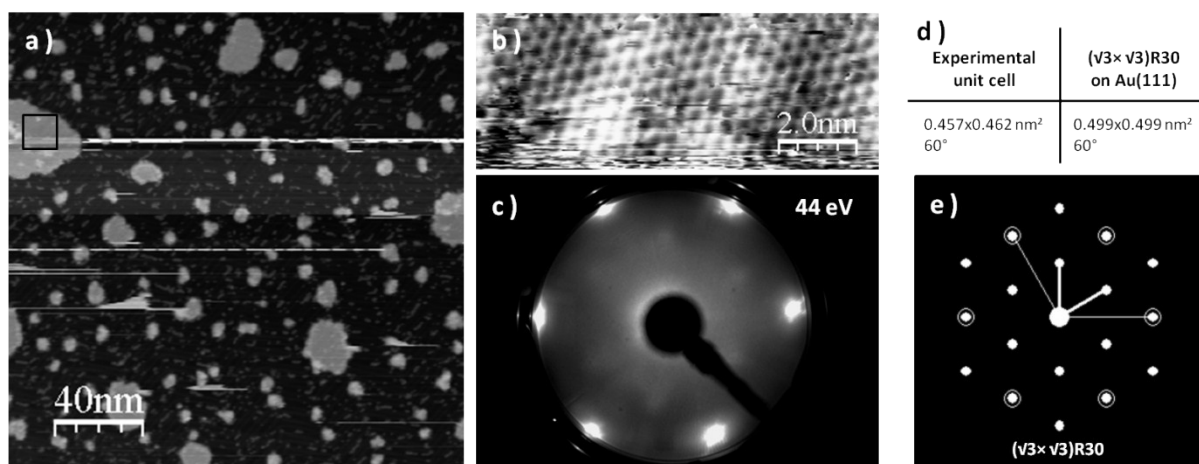


Fig. S1. Top and lateral views of (a) the Au<sub>3</sub>BMB<sub>3</sub> and (b) the BMB<sub>3</sub> relaxed structures.

**BMB 1.7 ML/h deposition on Au(111) held at 120K**



**Fig. S2.** STM topography after the deposition of BMB molecules at 120K, 200×200 nm<sup>2</sup>, V=600mV, I=25pA. The black square on the left side of the image corresponds to b) STM topography of a S island 10×4 nm<sup>2</sup>, V=-50mV, I=40pA c) LEED patterns; d) comparison chart for the experimental S unit cell and the simulated  $(\sqrt{3} \times \sqrt{3})R30$  unit cell on Au(111) (substrate unit vector 0.288 nm) e) simulated LEED pattern of the  $(\sqrt{3} \times \sqrt{3})R30$  unit cell on Au(111).

After the adsorption of BMB molecules on Au(111) at 120K and immediately cooled down to 4.3K it was possible to observe that an abnormal quantity of atomic sulfur coadsorbs on the surface (Figure S1a). The ratio BMB molecules to S is 1:98. The extra sulfur is presumably due to thermal degradation processes that occur in the crucible during the sublimation, indeed in this sample numerous BMB molecules are observed to adsorb without thiol groups. The latter are responsible for the formation of incomplete triangles as discussed in the main text. The sulfur islands do not affect the herringbone reconstruction of the Au surface (Figure S2b) and adopt a close packed hexagonal motif. By performing LEED analysis on this system (Figure S2c) it is possible to identify a  $(\sqrt{3} \times \sqrt{3})R30$  aggregation pattern on the surface of Au(111). The unit cell parameters extracted experimentally from the STM topographies (Figure S2d) display unit vectors 0.457x0.462 nm<sup>2</sup> and an angle of 60° between them. In good agreement with the simulation of a  $(\sqrt{3} \times \sqrt{3})R30$  obtained with the LeedPat software. In Figure S2e the simulation of the LEED pattern is reported.

XPS (Mg  $K\alpha$ ) on DTTP/Au(111)

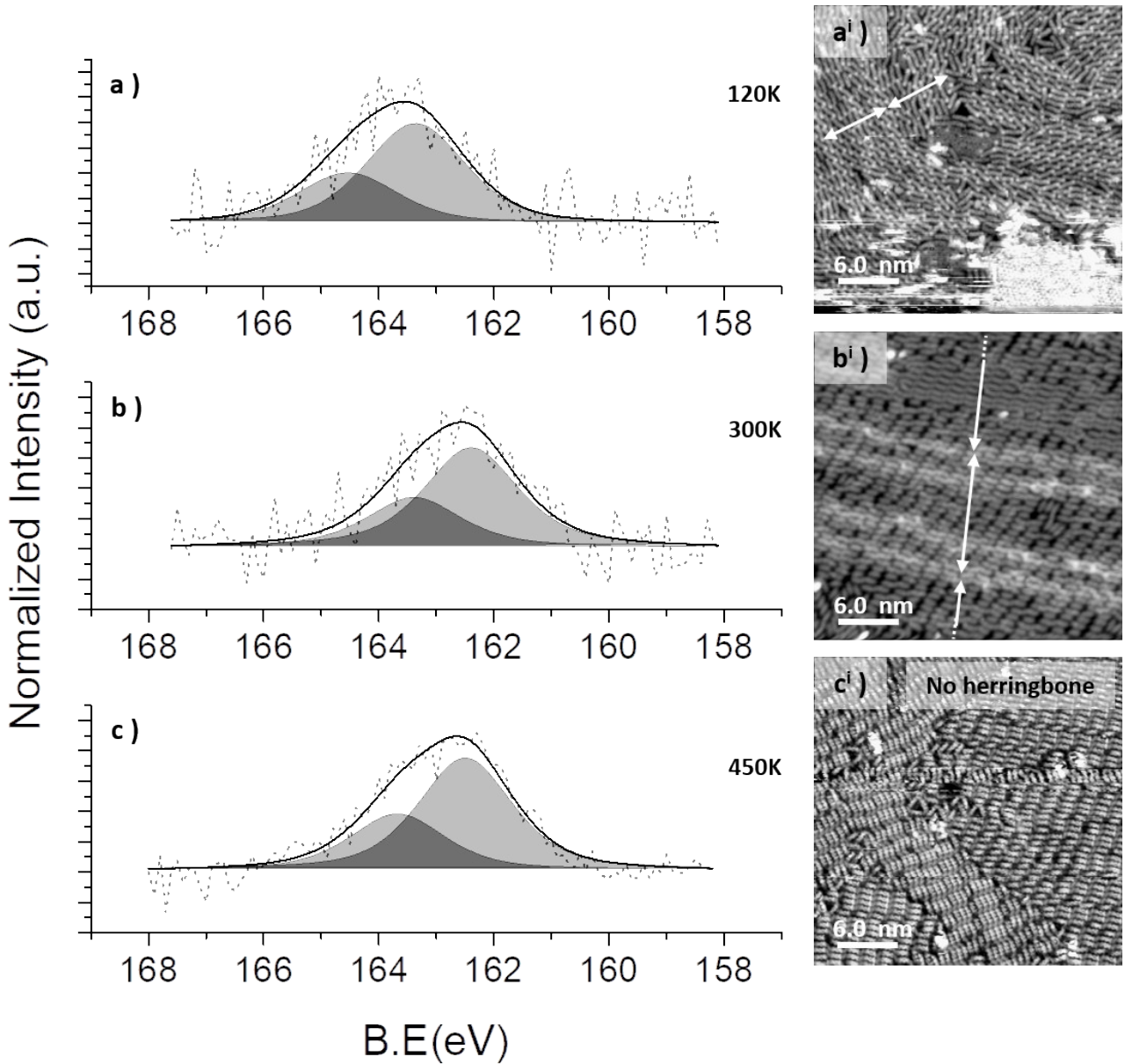


Fig. S3. Mg  $k_{\alpha}$  XPS spectra of S 2p acquired a) after deposition at 120K b) after RT thermalization and c) after annealing at 450K. The annealing steps were carried out on the same sample. S 2p 1/2 and 3/2 doublet fitted with a fixed energy separation of 1.18 eV. ai) STM topography  $30 \times 30 \text{ nm}^2$ ,  $V = -50 \text{ mV}$ ,  $I = 10 \text{ pA}$  for the system deposited at 120K and recorded at 4.3K bi) STM topography  $30 \times 30 \text{ nm}^2$ ,  $V = -50 \text{ mV}$ ,  $I = 80 \text{ pA}$  for the system thermalized at RT and recorded at 4.3K and ci) STM topography  $30 \times 30 \text{ nm}^2$ ,  $V = -50 \text{ mV}$ ,  $I = 100 \text{ pA}$  for the system annealed at 450K and recorded at 4.3K. The white arrows act as a guide to the eye denoting the herringbone reconstruction periodicity and revealing its enhancement as the Au adatom ablation sets in at 300 K.

The XPS analysis on the high molecular density sample, performed at different temperatures, reveal important changes relative to the S2p XPS signal. The as-deposited system at 120K reveals a S2p signal where the S 2p<sub>3/2</sub>

peak at 163.3 eV (Figure S3a) characteristic of physisorbed, or unbound thiol groups. In figure S3ai a representative STM topography is reported where it is possible to observe the unaffected herringbone pattern of the Au(111) surface, with a periodicity in the order of that of the pristine Au surface (6.3 nm). The sample annealed at RT shows the S 2p<sub>3/2</sub> peak locates at 162.4 eV (Figure S3b). A representative image for this system is displayed in Figure S3bi. The molecules now appear with dimmer termini following the chemisorption with the Au surface atoms. Occasionally, in this system, also wires of linear metal-organic Au-thiolates are found, which involve ablation of the Au-surface atoms. At this stage, a notable deformation of the Au(111) herringbone reconstruction is observed. The number of dislocations along the reconstruction lines is reduced. At the same time, the reconstruction's periodicity increases to tens of nm. Taking into account that the pristine herringbone reconstruction is formed by a high-density overlayer, Au atom ablation reduces its density and thus increases the reconstruction's periodicity. By further increasing the annealing temperature to 450K the XPS spectrum remains nearly unchanged (Figure S3c) and in the corresponding STM topography (Figure S3ci) it is possible to observe that the linear metal-organic complex are the dominant product. At this temperature it is also observed the onset of the formation of the triangular complexes and the herringbone reconstruction of the Au(111) is completely lost. By annealing over 500K the XPS spectra become heavily attenuated due to the substantial desorption of the molecular overlayer. Besides, the onset of side reactions (formation of thioethers)<sup>1</sup> and the broadening of the spectra makes the identification of the sulfur species via XPS analysis impossible.

---

<sup>1</sup>Rastgoo-Lahrood, A.; Martsinovich, N.; Lischka, M.; Eichhorn, J.; Szabelski, P.; Nieckarz, D.; Strunskus, T.; Das, K.; Schmittl, M.; Heckl, W. M.; et al. From Au-Thiolate Chains to ThioetherSierpiński Triangles: The Versatile Surface Chemistry of 1,3,5-Tris(4-Mercaptophenyl)Benzene on Au(111). *ACS Nano* **2016**, *10* (12), 10901–10911. <https://doi.org/10.1021/acsnano.6b05470>

Large scale STM images of the samples depicted in Fig. 2 of the main text.

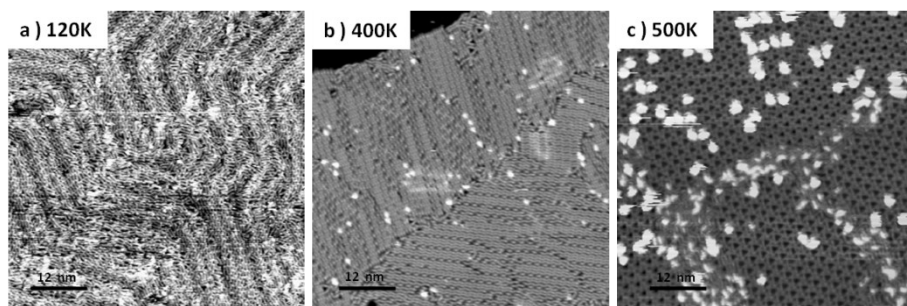


Fig. S4. Large scale ( $60 \text{ nm} \times 60 \text{ nm}$ ) of the same samples displayed in Fig. 2 of the main text, namely with full monolayer deposition on a substrate held at 120 K (a), the same sample after being heated to 400 K (b) and to 500 K (c).

Comparison of formation energies per molecule for different structures.

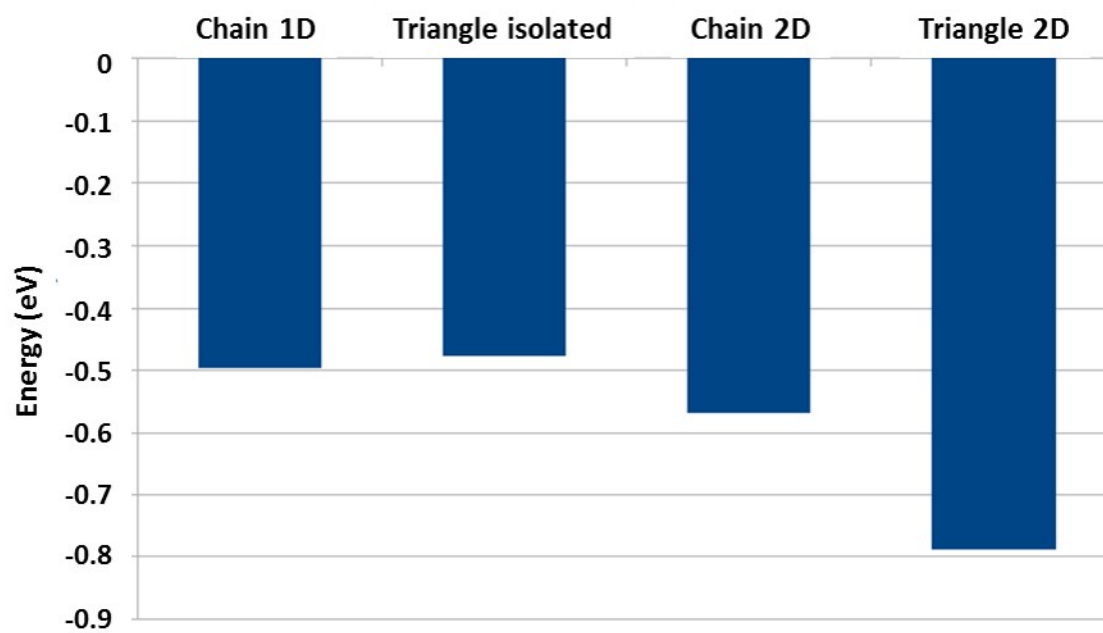


Fig. S5. Formation energies per molecule calculated by DFT for linear and triangular complexes as single entities, as well as in 2D assemblies.

### Geometries used in EBEM calculations

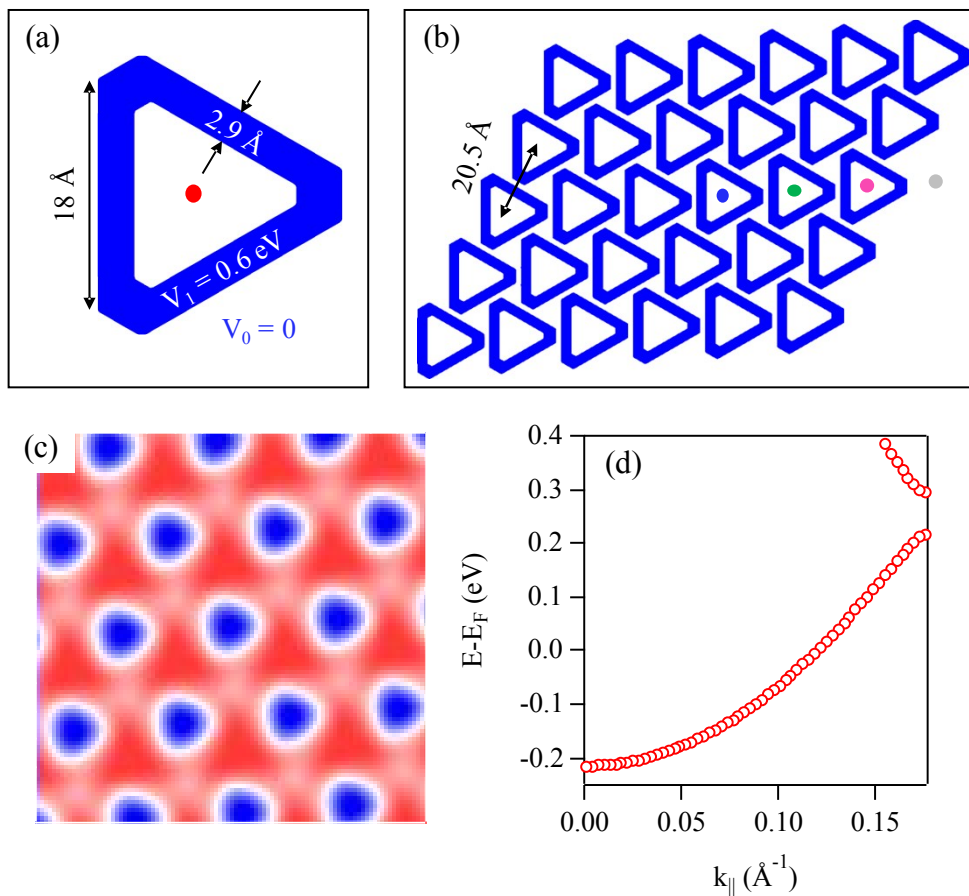


Fig. S6. The geometries used for EBEM calculations for the (a) Single triangle and (b) a 5x6 molecular island. The white background stands for the Au(111) substrate, while the blue segments define the molecular backbone with a scattering potential of 0.6 eV. The molecular size and periodicity are indicated on the figure. The circles in (b) mark the location at which the LDOSs presented in Fig. 4 is taken. (c) The 2D-LDOS for an infinite network taken at the resonance energy ( $E = 0.205 \text{ eV}$ ) (d) The EPWE-calculated surface state dispersion for an infinite triangle network, showing a 80 meV gap opening at the zone boundary.